Cytotoxic activity and cytostatic mechanism of novel 2-arylbenzo[b]furans

Hua Yang, Ji-Yan Pang, Yu-Chen Cai, Zun-Le Xu
and Li-Jian Xian

Abstract

The aims of this study were to screen cytotoxic compounds from 14 newly-synthesized 2-aryl-benzo[b]furans and explore their mechanisms of action. Cytotoxicity was determined by the MTT method. Cell-cycle distribution was detected by flow cytometry. Wright–Giemsa staining was performed to demonstrate the morphological features of cells in mitotic phase. Polymerization of tubulin was detected by tubulin assembly assay, and the cellular microtubule network was observed by immunocytochemical study. Among the 14 compounds screened, 4-formyl-2-(4-hydroxy-3-methoxyphenyl)-5-(2-methoxycarbonyethyl)-7-methoxy-benzo[b]furan (ERJT-12) showed significant cytotoxicity. Our results demonstrated that ERJT-12 exhibited anti-cancer activity in a variety of tumour cell lines with an IC50 value (concentration resulting in 50% inhibition of cell growth) of 5.75~17.29 μM. Cell cycle analysis showed a concentration-dependent accumulation of tumour cells in G2/M phase after treatment with ERJT-12. Further investigation indicated that ERJT-12 blocked the cell cycle in M phase, with separation and dispersion of chromosomes. ERJT-12 inhibited tubulin polymerization in-vitro. Changes of the cellular microtubule network caused by ERJT-12 were also detected, which were similar to the changes caused by colchicine. These results suggested that the anti-cancer activity of ERJT-12 is worth further investigation.

Introduction

Lignans and neolignans are a class of dibenzylbutane derivatives that exists in higher plants or can be synthesized (Singleton & Sainsbury 1987). These compounds possess a variety of biological actions, including anti-cancer, antimicrobial, immunomodulatory, anti-inflammatory and antioxidant activity (Hirano et al 1994; Wang et al 1995; Cho et al 1999; Pauletti et al 2000; Yu et al 2000; Kangas et al 2002; Piccinelli et al 2005). Benzo[b]furans are a prominent sub-group belonging to neolignans or nor-neolignans. It was reported that many benzofurans possess cytotoxic activity (Tsai et al 1996; Bohnenstengel et al 1999). Hayakawa et al (2004) demonstrated that several synthesized benzofuran derivatives exhibited highly potent cytotoxicity against a tumorigenic cell line. Li et al (2005) reported that two new benzofurans isolated from the seeds of *Styrax perkinsiae* exhibited significant cytotoxic activity against human breast cancer cell lines MCF-7 and MDA-MB-231. In addition, benzofurans display other biological actions, such as oestrogenic (Halabalaki et al 2000), anti-angiogenic (Apers et al 2002), antithrombotic (Ma et al 1993) and antioxidant (Maeda et al 1994) activity.

In this study, a total of 14 synthesized 2-arylbenzo[b]furans (Table 1) were screened for their cytotoxic activity against human tumour cells; among them compound ERJT-12 was found to exhibit prominent cytotoxic effect. The cytotoxic mechanisms were related to the inhibition of tubulin polymerization.

Materials and Methods

Synthesis of 2-arylbenzo[b]furans

A series of 2-arylbenzo[b]furans was synthesized at the Department of Chemistry, Sun Yat-Sen University using the method described by Yang et al, adopting Castro's route

State Key Laboratory of Oncology in Southern China, Cancer Center, Sun Yat-sen University, Guangzhou, P. R. China
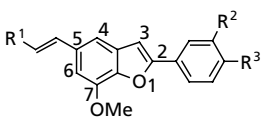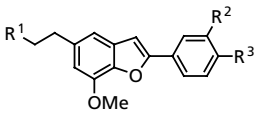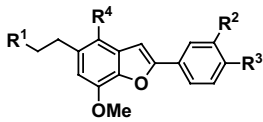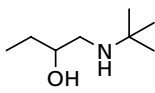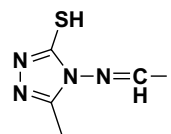
Hua Yang, Yu-Chen Cai, Li-Jian Xian

School of Chemistry and Chemical Engineering, Sun Yat-sen University, Guangzhou, P. R. China

Ji-Yan Pang, Zun-Le Xu

Correspondence: L.-J. Xian, Cancer Center, Sun Yat-sen University, Guangzhou, 510060, P. R. China.
E-mail: lj_xian@yahoo.com

Table 1   Structure of the synthetic 2-arylbenzo[b]furans

	Compound	R^1	R^2	R^3	R^4
	PJY-02	HOCO-	–	Cl-	–
	PJY-04	HOCH$_2$-	–	Cl-	–
	ERJT-01	CH$_3$OCO-	CH$_3$O-	PhCH$_2$O-	–
	ERJT-21	HOCH$_2$-	CH$_3$O-	PhCH$_2$O-	–
	ERJT-06	NH$_2$CO-	CH$_3$O-	OH-	–
	ERJT-09	HOCO-	CH$_3$O-	OH-	–
	ERJT-16	HOCH$_2$-	CH$_3$O-	OH-	–
	ERJT-18	CH$_3$OCO-	CH$_3$O-	(structure)	–
	ERJT-23	HOCH$_2$-	CH$_3$O-	CH$_3$O-	–
	ERJT-12	CH$_3$OCO-	CH$_3$O-	OH-	CHO-
	ERJT-26	CH$_3$OCO-	CH$_3$O-	OH-	HOCH$_2$-
	ERJT-28	HOCO-	CH$_3$O-	OH-	CHO-
	ERJT-29	CH$_3$OCO-	CH$_3$O-	OH-	(triazole structure)
	ERJT-30	CH$_3$OCO-	OH-	OH-	CHO-

(Yang et al 1992). Details of the synthesis and confirmation of the compounds have been reported elsewhere (Pang et al 2005). In brief, coupling reaction of a cuprous acetylide with phenyl bromide yielded compound ERJT-01. PJY-02 was produced through the hydroxylysis of 5-(2-methoxycarbonyl)-*trans*-ethenyl)-7-methoxy-2-(4-chlorophenyl)benzo[b]furan (I) prepared from coupling reaction of another cuprous acetylide with phenyl bromide. ERJT-21 and PJY-04 were obtained in a high yield via hydrogenolysis of ERJT-01 and I, respectively, in the presence of LiAlH$_4$ catalysis. Hydrogenolysis of ERJT-01 in the presence of hydrogen under Pd/C produced 5-(2-methoxy-carbonyl)ethyl)-7-methoxy-2-(3-methoxy-4-hydroxyphenyl)lbenzo-[b]furan (II). An amide, ERJT-06, was readily prepared from the reaction of compound II with 28% ammonia solution. Vilsmeier reaction and hydrogenolysis of II afforded C-4 formylated products ERJT-12 and ERJT-16 as the main products. Methylation of ERJT-16 with iodomethane gave compound ERJT-23 under KF/Al$_2$O$_3$ catalysis. ERJT-18 was made from amination reaction of *tert*-butylamine and III obtained from alkylation reaction of II with epichlorohydrin. Hydrogenolysis, hydroxylysis, part demethylation and a reaction with 1-amino-2-methyl-5-mercapto-1*H*-1,3,5-triazole of ERJT-12 gave, respectively, compounds ERJT-26, ERJT-28, ERJT-30 and ERJT-29. All the synthetic compounds were fully characterized by MS, ^{1}HNMR, IR and elemental analysis.

Reagents

All the synthetic compounds were dissolved in DMSO at 10 mg mL^{-1} as stock solution. Dilution was made in culture medium before use. Colchicine was purchased from Calbiochem (San Diego, CA) and dissolved in 0.9% NaCl. Equal volumes of solvents were used in the control experiments. Anti-β-tubulin antibody was purchased from NeoMarkers (Fremont, CA). Fluorescent isothiocyanate-conjugated secondary antibody was purchased from SouthernBiotech (Birmingham, AL). Cell-culture reagents were obtained from Invitrogen (Carlsbad, CA).

Cell lines

Human oral carcinoma KB-3-1 cells, gastric carcinoma MGC803 cells, lung adenocarcinoma GLC82 cells, cervical epitheloid carcinoma HeLa cells and human bladder carcinoma cell line ECV-304 were maintained in RPMI 1640 supplied with 10% newborn calf serum at 37°C under 5% CO$_2$; human breast carcinoma MCF-7 cells were cultured in DMEM with 10% newborn calf serum. Human T-lymphoblastic leukemia CCRF/CEM cells were kindly provided by Professor Hans Grunicke (Institute of Medical Chemistry and Biochemistry, Innsbruck University, Austria), and were maintained in RPMI 1640 supplied with 10% newborn calf serum.

Growth inhibition assay

In-vitro growth inhibition effect of the synthetic compounds was determined by MTT assay. In brief, cells in the logarithmic phase were seeded into 96-well microplates and exposed to various compounds at 37°C for 72 h.

At the end of drug exposure, 20 μL of 5 mg mL^{-1} 3-(4,5-dimethylthiazol-2-yl)-2,5-diphenyltetrazolium bromide (MTT) solution was directly added to each cell culture well and the plates were incubated at 37°C for 4 h. The formazan converted from tetrazolium salt by viable cells was solubilized by 200 μL dimethyl sulfoxide, and measured in a microplate reader (Thermo Labsystems, Franklin, MA) at 570 nm. The IC50 value resulting from 50% inhibition of cell growth was calculated as a comparison with the control.

Flow cytometric analyses of apoptosis and cell cycle

MCF-7 cells were incubated with various concentrations of ERJT-12 for 24 h, then cells were harvested and washed with phosphate-buffered saline (PBS) and fixed in ice-cold 70% ethanol overnight. The fixed cells were incubated with 5 μg mL^{-1} Rnase I and 1 μg mL^{-1} propidium iodide. Cellular DNA content was determined by a flow cytometer (Beckman Coulter, Fullerton, CA). At least 10 000 cells of each sample were analysed. Apoptotic cells were observed in the cell-cycle distribution. Cell-cycle analysis was also simultaneously performed.

Morphology and mitotic index assays

After 24 h of treatment by various concentrations of ERJT-12, MCF-7 cells were harvested and smeared on slides. The slides were air dried, fixed in methanol–acetone (3:1 v/v), and stained with Giemsa at room temperature for 15 min. Alterations of nuclei, membranes and morphological features were observed by light microscopy. Cells in mitotic phase were recognized by the appearance of chromosomes dispersed in the cytoplasm and by the disappearance of nuclear membranes. Mitotic cells were scored by randomly counting 200 cells by light microscopy to calculate the mitotic index (%).

Inhibition assay of tubulin assembly

Purified tubulin from calf brain was purchased from Cytoskeleton, Inc. (Denver, CO). The effects of ERJT-12 on the microtubule assembly process were determined using the conditions recommended by the manufacturer. For assembly inhibition, 100 μL of tubulin solution (10 mg protein/mL) were mixed gently with 400 μL of reaction buffer containing 80 mM PIPES (pH 6.9), 1.0 mM MgCl$_2$, 1.0 mM EGTA, and 10% glycerol. ERJT-12 (final concentration of 5 μM and 10 μM, respectively) or colchicine (final concentration of 5 μM) was then added to the sample cuvette. After adding GTP to the sample to a final concentration of 1.0 mM, the microtubule assembly process was monitored by measuring the change of optical density at 37°C at 340 nm every 5 min on a spectrophotometer (Beckman Coulter, Fullerton, CA) until the assembly process was completed, usually within 45 min.

Immunocytochemical study

MCF-7 cells plated on coverslips were treated with different concentrations of ERJT-12 for 12 h. Colchicine and paclitaxel were included as control. After treatment, cells were fixed with cold methanol at −20°C for 10 min, and washed with PBS solution. Then cells were blocked with 3% bovine serum albumin in PBS for 30 min and further incubated with monoclonal anti-β-tubulin antibody at room temperature for 2 h. After being washed with PBS solution, cells were re-incubated with fluorescein isothiocyanate-conjugated second antibody in a dark room for 1 h at room temperature. Cellular microtubules were observed with an Olympus IX70 fluorescence microscope.

Statistical analysis

All data were repeated at least three times in independent experiments. Statistical analysis of the cytotoxic effect (IC50) of ERJT-12 on different cancer cell lines was performed using the Kruskal–Wallis test (non-parametric). The effects of increasing concentrations of ERJT-12 (0, 5, 10, 15, 20 μM) on the cell cycle distribution and the mitotic index (%) were evaluated using the Kruskal–Wallis test (non-parametric). The effect of ERJT-12 and colchicine on tubulin polymerization was statistically examined using Friedman's test. In all cases, post-hoc comparisons of the means of individual groups were performed using Student–Newman–Keuls test. $P < 0.05$ denoted significance in all cases.

Results

Cytotoxicity of the compounds on human tumour cell lines

Table 2 shows the IC50 values of the 14 compounds in three human tumour cell lines. Among these compounds, ERJT-12 showed powerful anti-cancer activity. ERJT-18 and ERJT-30 were less effective than ERJT-12. Other compounds displayed minor cytotoxicity in human tumour cells. The IC50 values of ERJT-12 tested in different cancer cell lines are presented in Table 3. These cell lines showed different susceptibility to ERJT-12 ($\chi^2 = 18.320$, $P = 0.005$). Human breast carcinoma MCF-7 cells exhibited the highest susceptibility to ERJT-12, with an IC50 of ~5.8 μM, whereas ECV304 cells displayed the lowest susceptibility to ERJT-12 with an IC50 of ~17 μM ($P < 0.05$).

Effect of ERJT-12 on cell cycle

After 24 h of drug treatment, MCF-7 cells were analysed for their cell cycle. As shown in Table 4, untreated MCF-7 cells showed classical pattern of proliferating cells proportionally distributed in G$_0$/G$_1$ (50%), S (33%) and G$_2$/M (15%) phases.

Table 2 Cytotoxicity of the synthetic 2-arylbenzo[b]furans

Compounds	IC50 (μM)		
	KB-3-1	MGC803	GLC82
PJY-02	NA	NA	NA
PJY-04	NA	NA	NA
ERJT-01	NA	NA	NA
ERJT-06	> 50	> 50	47.76 ± 1.93
ERJT-09	> 50	> 50	> 50
ERJT-12	6.75 ± 0.68	9.30 ± 0.88	15.18 ± 1.56
ERJT-16	38.82 ± 1.74	30.18 ± 1.22	47.72 ± 2.92
ERJT-18	29.52 ± 1.71	28.08 ± 1.63	26.64 ± 0.95
ERJT-21	> 50	> 50	> 50
ERJT-23	> 50	> 50	> 50
ERJT-26	47.55 ± 1.48	49.29 ± 1.61	> 50
ERJT-28	> 50	> 50	> 50
ERJT-29	> 50	> 50	> 50
ERJT-30	26.30 ± 1.65	24.71 ± 1.76	26.08 ± 1.62

Cell survival was determined by MTT assay. IC50 value was calculated as described in Materials and Methods. Each value represents the mean ± s.d. of three independent experiments. NA, not available due to the poor solubility.

Table 3 ERJT-12-induced cytotoxicity in human tumour cell lines

Cell Type	Cell Line	IC50 (μM)
Breast cancer	MCF-7	5.75 ± 0.38
Oral carcinoma	KB-3-1	6.75 ± 0.68
Gastric cancer	MGC803	9.30 ± 0.88
Lung cancer	GLC82	15.18 ± 1.56
Cervical cancer	HeLa	8.65 ± 0.23
Bladder cancer	ECV-304	17.29 ± 1.64
T-cell leukaemia	CCRF/CEM	8.82 ± 0.37

Cell survival was determined by MTT assay. IC50 value was calculated as described in Materials and Methods. Each value represents the mean ± s.d. of three independent experiments. MCF-7 cells exhibited the highest susceptibility to ERJT-12, whereas ECV304 cells displayed the lowest susceptibility to ERJT-12 ($P < 0.05$).

Table 4 Blocking of cell cycle at G_2/M phase by ERJT-12 in MCF-7 cells

Concentration (μM)	G1 (%)	S (%)	G2/M (%)	Apoptosis (%)
Control	48.7 ± 6.2	33.4 ± 4.3	18.0 ± 3.1	2.3 ± 0.8
5	47.7 ± 5.1	31.0 ± 3.3	24.6 ± 3.9	5.7 ± 0.8*
10	24.5 ± 2.3*	37.4 ± 3.7	38.1 ± 2.8*	11.3 ± 1.9*
15	19.0 ± 3.0*	37.0 ± 4.6	44.0 ± 6.3*	12.3 ± 2.5*
20	17.9 ± 2.5*	33.5 ± 3.8	48.6 ± 6.6*	6.2 ± 1.1*

Cell cycle analysis was performed as described in Materials and Methods. Each point represents the mean ± s.d. of three independent experiments. *$P < 0.05$ compared with the control group.

ERJT-12 treatment induced an accumulation of MCF-7 cells in G_2/M phase ($\chi^2 = 12.433$, $P = 0.014$), and higher concentrations of ERJT-12 (10, 15, 20 μM) yielded relatively stronger arrest effect than lower concentration of ERJT-12 (5 μM) did ($P < 0.05$). Concurrently, losses of cells from G_1 phase were observed after the treatment of ERJT-12 ($\chi^2 = 12.233$, $P = 0.016$), and there was more remarkable reduction of G_1 cells in groups of higher concentrations (10, 15, 20 μM ERJT-12) than in the group of lower concentration (5 μM ERJT-12) ($P < 0.05$). No change of S phase was observed ($\chi^2 = 5.151$, $P > 0.05$). ERJT-12 treatment also induced obvious apoptosis in MCF-7 cells ($\chi^2 = 12.433$, $P = 0.014$). The increment of sub-G_1 cells reached a zenith at the concentration of 10 and 15 μM ERJT-12, then decrement of sub-G_1 cells occurred although the concentration increased ($P < 0.05$). Similar results were obtained with MGC803 cells (data not shown).

Mitotic arrest

MCF-7 cells were arrested in metaphase after treatment with ERJT-12 for 24 h. The cells possessed intact plasma membranes but nuclear membranes were absent. The chromosomes were loosely separated and dispersed in the cytoplasm (Figure 1B), whereas intact nuclei were seen in control cells (Figure 1A). For quantitative analysis of mitotic arrest, the percentage of cells arrested in mitosis was calculated by counting at least 200 cells. ERJT-12 induced significant increment of mitotic cells ($\chi^2 = 13.500$, $P = 0.000$). Approximately 3% of cells were at M phase in the control group. In the presence of 5, 10, 15, 20 μM of ERJT-12, the mitotic index was 10.8 ± 1.8%, 33.7 ± 2.1%, 26.3 ± 2.1% and 21.3 ± 1.5%, respectively ($P < 0.05$).

Effect of ERJT-12 on tubulin polymerization in-vitro

Because ERJT-12 treatment markedly blocked the cell cycle in the M phase, we were interested in whether ERJT-12 could inhibit tubulin polymerization. As shown in Figure 2, the tubulin assembly process was inhibited by ERJT-12 and colchicine when compared with the control sample ($\chi^2 = 15.240$, $P = 0.001$). Statistical analysis showed that 5 μM of ERJT-12 displayed little inhibitory effect on tubulin polymerization ($P > 0.05$). In the presence of 10 μM ERJT-12, tubulin polymerization was significantly inhibited compared with that of the control sample. Colchicine (5 μM) showed the most potent inhibitory effect on tubulin polymerization ($P < 0.05$).

Effect of ERJT-12 on cellular microtubules

Because strong colchicine-like tubulin-destabilizing activity was found in-vitro, we further examined the effect of ERJT-12 on the cellular microtubule network by immunocytochemistry. The microtubule network in control cells exhibited normal arrangement and organization (Figure 3A). Treatment with colchicine caused cellular microtubule depolymerization with short microtubules in the cytoplasm (Figure 3C). The findings in ERJT-12-treated cells were similar to those of colchicine-induced microtubule changes (Figure 3B). In contrast,
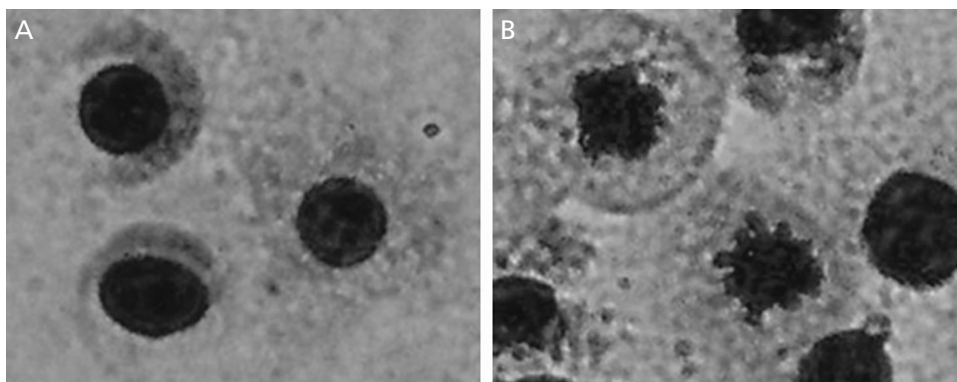
Figure 1 Morphological examination of ERJT-12-induced M-phase arrest in MCF-7 cells. MCF-7 cells were treated with 5 μM ERJT-12 or with the same volume of solvent as control. After 24 h of treatment, cells were harvested and stained with Giemsa. In ERJT-12-treated cells ($\times$ 300), typical metaphase arrest cells presented with condensed and separated chromosomes (B), whereas control cells ($\times$ 300) were in interphase with intact nuclei (A).
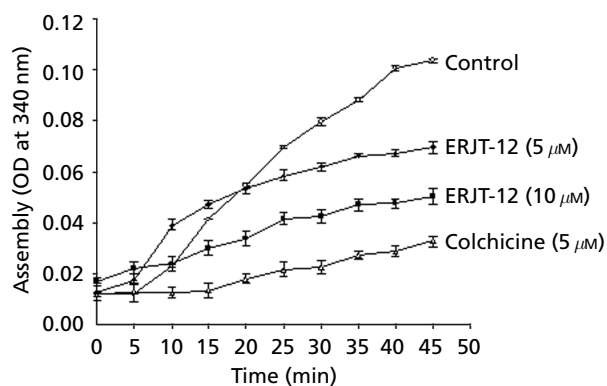

Figure 2 Inhibition of microtubule assembly by ERJT-12 in-vitro. Purified bovine tubulin in a reaction buffer was incubated at 37°C in the presence of 5 μM, 10 μM ERJT-12 and the same volume of solvent as control. Colchicine (5 μM) was used as a positive control. Tubulin polymerization was determined by measuring absorbance at 340 nm. Each point represents the mean $\pm$ s.d. of three independent experiments. 5 μM of ERJT-12 had no inhibitory effect on tubulin polymerization ($P > 0.05$). In the presence of 10 μM ERJT-12 or 5 μM of colchicine, tubulin polymerization was significantly inhibited compared with that of the control sample ($P < 0.05$).

paclitaxel treatment caused microtubule polymerization with an increase in the density of cellular microtubules and formation of thick microtubule bundle surrounding the nucleus (Figure 3D).

Discussion

In this study, we found that although all 14 compounds possessed the same 2-arylbenzofuran skeleton, they were very different in their cytotoxic activity. This indicated that the different sub-groups of these compounds were closely related to the cytotoxicity. The preliminary structure–activity relationships could be obtained from our results. Firstly, when the substituent was a propionic methyl ester at C-5, a

formyl at C-4 increased cytotoxicity remarkably (ERJT-12 and ERJT-30). However, the potency became worse when the formyl was changed to alcohol (ERJT-26) or other substituents containing nitrogen (ERJT-29). Secondly, the 3-methoxy-4-hydroxyphenyl at C-2 contributed more potent cytotoxicity to ERJT-12 than catechol did to ERJT-30. Finally, the ethylenic link at C-5 might be related to the poor solubility of the compounds (PJY-02, PJY-04 and ERJT-01).

Cell-cycle analysis showed a significant accumulation of G_2/M cells induced by ERJT-12, concurrent with a reduction of cells in G_1 phase. M-phase block was further examined using morphological criteria. It was found that up to 34% of ERJT-12-treated cells were full of scattered metaphase chromosomes in the cytoplasm. This indicates that the G_2/M accumulation was partly due to the blockage of M-phase cells.

Microtubules play a crucial role during mitosis. Disruption of the microtubule can trigger the cell-cycle checkpoint and induce M-phase arrest. Cell-cycle checkpoints refer to the regulatory pathways that restrain cell-cycle transitions in response to stress. These pathways coordinate cell-cycle transitions and ensure faithful replication of the genome before cell division (Paulovich et al 1997). Cells can arrest transiently at cell-cycle checkpoints to allow for the repair of cellular damage. Alternatively, if damage is irreparable, checkpoint signalling might activate pathways that lead to programmed cell death. There are three kinds of checkpoints during the cell cycle — DNA damage checkpoint, DNA replication checkpoint and mitotic spindle checkpoint. The mitotic spindle checkpoint monitors the microtubule structure and chromosome attachments of the mitotic spindle and delays chromosome segregation during mitosis until defects of the mitotic spindle apparatus are corrected (Musacchio & Hardwick 2002; Stewart et al 2003). Microtubule inhibitors, such as colchicine (Rowinsky & Donehower 1991), prevent the formation of mitotic spindles by inhibiting the assembly of microtubule from tubulins, thus triggering the spindle checkpoint and arrest cell cycle in M phase. In this study, we hypothesized that ERJT-12 could directly affect tubulin. Using tubulin assembly assay we found that ERJT-12
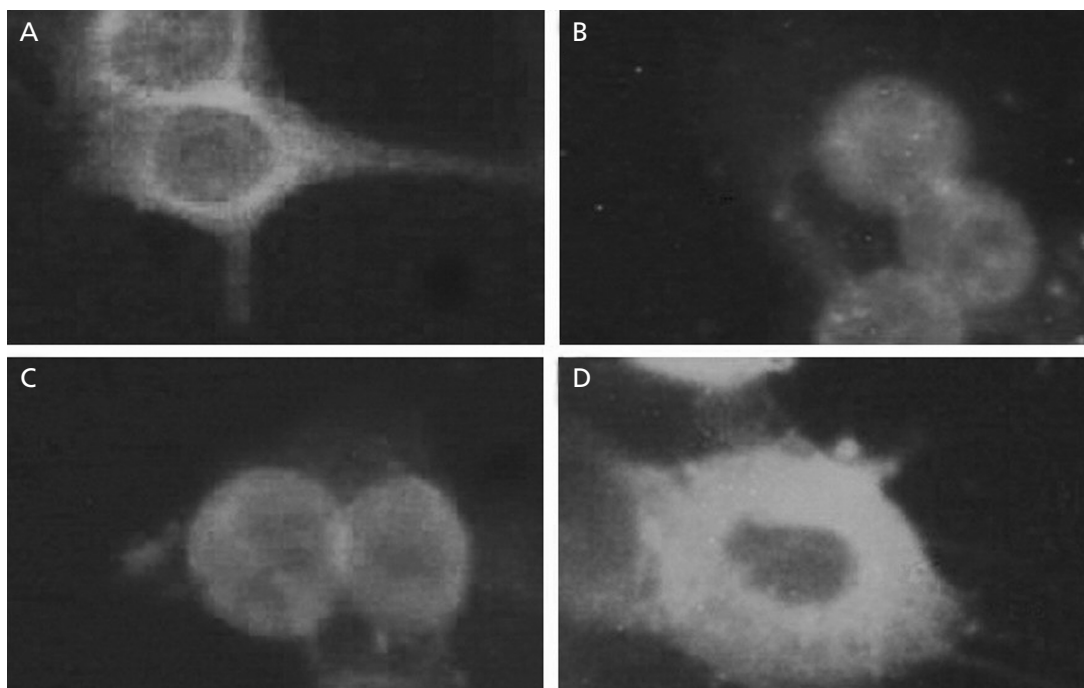
Figure 3 Effect of ERJT-12 on cellular microtubule organization. MCF-7 cells were treated with different drugs respectively, or with the same volume of solvent as control. After a 12-h incubation, cellular microtubules were visualized ($\times$ 300) with indirect immunofluorescence techniques using a monoclonal β-tubulin antibody. A. Control. B. ERJT-12 (5 μM). C. Colchicine (0.5 μM). D. Paclitaxel (0.5 μM).

inhibited the polymerization of tubulin in the cell-free system, which was similar to the effect of colchicine treatment. To further confirm the results, changes in the cellular microtubule network were observed by an immunocytochemical study. It was found that the effect of ERJT-12 was similar to that of colchicine but different from that of paclitaxel. Shortened depolymerized microtubules were observed in ERJT-12- and colchicine-treated cells, whereas thick bundles of microtubule network surrounding the nucleus were seen in paclitaxel-treated cells.

In conclusion, among the 14 2-arylbenzo[b]furans screened, ERJT-12 was found to possess potent activity in suppressing the proliferation of various human tumour cells. Our study demonstrated that ERJT-12 inhibited microtubule assembly and suspended the cell cycle at the M phase. There is justification for the development of this new lignan compound as a potential anti-cancer agent.

References

Apers, S., Paper, D., Burgermeister, J., Baronikova, S., Van Dyck, S., Lemiere, G., Vlietinck, A., Pieters, L. (2002) Antiangiogenic activity of synthetic dihydrobenzofuran lignans. *J. Nat. Prod.* **65**: 718–720

Bohnenstengel, F. I., Steube, K. G., Meyer, C., Quentmeier, H., Nugroho, B. W., Proksch, P. (1999) 1H-cyclopenta[b]benzofuran lignans from Aglaia species inhibit cell proliferation and alter cell cycle distribution in human monocytic leukemia cell lines. *Z. Naturforsch. [C]* **54**: 1075–1083

Cho, J. Y., Kim, A. R., Yoo, E. S., Baik, K. U., Park, M. H. (1999) Immunomodulatory effect of arctigenin, a lignan compound, on tumour necrosis factor-alpha and nitric oxide production, and lymphocyte proliferation. *J. Pharm. Pharmacol.* **51**: 1267–1273

Halabalaki, M., Aligiannis, N., Papoutsi, Z., Mitakou, S., Moutsatsou, P., Sekeris, C., Skaltsounis, A. L. (2000) Three new arylobenzofurans from Onobrychis ebenoides and evaluation of their binding affinity for the estrogen receptor. *J. Nat. Prod.* **63**: 1672–1674

Hayakawa, I., Shioya, R., Agatsuma, T., Furukawa, H., Naruto, S., Sugano, Y. (2004) A library synthesis of 4-hydroxy-3-methyl-6-phenylbenzofuran-2-carboxylic acid ethyl ester derivatives as anti-tumor agents. *Bioorg. Med. Chem. Lett.* **14**: 4383–4387

Hirano, T., Gotoh, M., Oka, K. (1994) Natural flavonoids and lignans are potent cytostatic agents against human leukemic HL-60 cells. *Life Sci.* **55**: 1061–1069

Kangas, L., Saarinen, N., Mutanen, M., Ahotupa, M., Hirsinummi, R., Unkila, M., Perala, M., Soininen, P., Laatikainen, R., Korte, H., Santti, R. (2002) Antioxidant and antitumor effects of hydroxy-matairesinol (HM-3000, HMR), a lignan isolated from the knots of spruce. *Eur. J. Cancer Prev.* **11** (Suppl.): S48–S57

Li, Q. L., Li, B. G., Qi, H. Y., Gao, X. P., Zhang, G. L. (2005) Four new benzofurans from seeds of Styrax perkinsiae. *Planta Med.* **71**: 847–851

Ma, Y., Han, G. Q., Wang, Y. Y. (1993) PAF antagonistic benzofuran neolignans from Piper kadsura. *Yao Xue Xue Bao* **28**: 370–373

Maeda, S., Masuda, H., Tokoroyama, T. (1994) Studies on the preparation of bioactive lignans of oxidative coupling reaction. I. Preparation and lipid peroxidation inhibitory effect of benzofuran lignans related to schizotenuins. *Chem. Pharm. Bull. (Tokyo)* **42**: 2500–2505

Musacchio, A., Hardwick, K. G. (2002) The spindle checkpoint: structural insights into dynamic signalling. *Nat. Rev. Mol. Cell Biol.* **3**: 731–741

Pang, J. Y., Wang, B., Chen, Z. P., Xu, Z. L. (2005) Synthesis of 2-arylbenzo[b]furan derivatives. *Chin. J. Org. Chem.* **25**: 176–181

Pauletti, P. M., Araujo, A. R., Young, M. C., Giesbrecht, A. M., Bolzani, V. D. (2000) nor-Lignans from the leaves of Styrax ferrugineus (Styracaceae) with antibacterial and antifungal activity. *Phytochemistry* **55**: 597–601

Paulovich, A. G., Toczyski, D. P., Hartwell, L. H. (1997) When checkpoints fail. *Cell* **88**: 315–321

Piccinelli, A. L., Mahmood, N., Mora, G., Poveda, L., De Simone, F., Rastrelli, L. (2005) Anti-HIV activity of dibenzylbutyrolactone-type lignans from Phenax species endemic in Costa Rica. *J. Pharm. Pharmacol.* **57**: 1109–1115

Rowinsky, E. K., Donehower, R. C. (1991) The clinical pharmacology and use of antimicrotubule agents in cancer chemotherapeutics. *Pharmacol. Ther.* **52**: 35–84

Singleton, P., Sainsbury, D. (1987) *Dictionary of microbiology and molecular biology*. 2nd Edn, Wiley, New York

Stewart, Z. A., Westfall, M. D., Pietenpol, J. A. (2003) Cell-cycle dysregulation and anticancer therapy. *Trends Pharmacol. Sci.* **24**: 139–145

Tsai, I. L., Hsieh, C. F., Duh, C. Y. (1996) Additional cytotoxic neolignans from Persea obovatifolia. *Phytochemistry* **43**: 1261–1263

Wang, J. P., Ho, T. F., Chang, L. C., Chen, C. C. (1995) Anti-inflammatory effect of magnolol, isolated from Magnolia officinalis, on A23187-induced pleurisy in mice. *J. Pharm. Pharmacol.* **47**: 857–860

Yang, Z., Liu, H. B., Lee, C. M., Chang, H. M., Wong, H. N. C. (1992) Regioselective introduction of carbon-3 substituents to 5-alkyl-7-methoxy-2-phenylbenzo[b]furans: synthesis of a novel adenosine A1 receptor ligand and its derivatives. *J. Org. Chem.* **57**: 7248–7257

Yu, Y. U., Kang, S. Y., Park, H. Y., Sung, S. H., Lee, E. J., Kim, S. Y., Kim, Y. C. (2000) Antioxidant lignans from Machilus thunbergii protect CCl4-injured primary cultures of rat hepatocytes. *J. Pharm. Pharmacol.* **52**:1163–1169